Title

Improved regressions with convolutional neural networks for surface enhanced Raman scattering sensing of metabolite biomarkers

ISBN

9781510628717

Authors

Thrift, William J

Nguyen, Cuong Q

Wang, Junlin

et al.

Publication Date

2019-09-03

DOI

10.1117/12.2535410

Improved Regressions with Convolutional Neural Networks for Surface Enhanced Raman Scattering Sensing of Metabolite Biomarkers

William John Thrift*, Cuong Quoc Nguyen*, Junlin Wang †, Jason Ernest Kahn †, Ruijun Dong †, Andrew Benjamin Laird †, Regina Ragan*

*Department of Materials Science and Engineering, University of California, Irvine

† Department of Information and Computer Science, University of California, Irvine,

ABSTRACT

Surface enhanced Raman scattering (SERS) is a vibrational spectroscopy method that enables the quantification of the concentration of small molecules. SERS sensing has been demonstrated in a wide variety of applications, from explosive and drug detection, to monitoring of bacteria growth. Underpinning SERS sensing are the sensor surfaces that are composed of vast quantities of metal nanostructures which confine light into small gaps called "hotspots", enhancing Raman scattering. While these surfaces are essential for increasing Raman scattering intensity so that analyte signal may be observed in small concentrations, they introduce signal variations due to spatial distributions of Raman enhancement and hotspot volume. In this work, we introduce a convolutional neural network model that improves concentration regressions in SERS sensors by learning the distributions of sensor surface dependent latent variables. We demonstrate that this model significantly improves predictions compared to a traditional multilayer perceptron approach, and that the model uses analyte spectral information and is capable of reasonable interpolations.

Keywords: SERS, Self-Assembly, Machine Learning, Sensing, Convolutional Neural Network

INTRODUCTION

Vibrational spectroscopies hold enormous promise as chemosensors due to the "fingerprint" spectral region – roughly from 400 cm^{-1} to 1700 cm^{-1} – that can be used to uniquely identify small molecules. Yet traditional vibrational spectroscopies like infrared spectroscopy and Raman spectroscopy have insufficiently large adsorption and scattering crossections, respectively, for use in sensing at small concentrations.[1] Surface enhanced Raman spectroscopy (SERS) has emerged as a promising method for enhancing Raman scattering to the point where small concentrations of analyte molecules can be quantified.[2] SERS relies on the near electric field enhancement of light due to scattering with metal nanostructures,[3] which can result in increases in Raman scattering by factors as large as 10^9.[4]

SERS has many attractive qualities for sensing. Large SERS EFs eschew the need for labeled detection schemes as even nonresonant molecules with small Raman cross-sections can be directly sensed.[5] SERS has been used for the detection of explosives,[6] drugs,[7] and toxins.[8] Additionally, the fingerprint spectral window enables highly multiplexed sensing.[9] Finally, SERS surfaces enable real time, in-line measurements for longitudinal monitoring of molecules, making it ideal for monitoring infections.[10]

Fabrication methods compatible with nanomanufacturing, specifically chemical self-assembly, have advanced to the point where the sub-nanometer gaps between nanostructures used in SERS can be reliably produced.[11–14] In the context of plasmonics these gaps, called hotspots, yield unprecedented enhancements of light matter interactions.[15] We have recently demonstrated a chemical assembly method – 2-dimensional

Nanoengineering: Fabrication, Properties, Optics, Thin Films, and Devices XVI,
edited by Balaji Panchapakesan, André-Jean Attias, Proc. of SPIE Vol. 11089,
1108907 · © 2019 SPIE · CCC code: 0277-786X/19/$21 · doi: 10.1117/12.2535410

physically activated chemistry (2PAC) – capable of obtaining a SERS EF exceeding 10^9 with just 10% relative standard deviation over a 1 mm^2 area.[16] This advance has enabled the collection of large, uniform datasets that enable a big data, machine learning approach to SERS sensing.[17] Traditional methods of calibrating SERS surfaces' quantitative response only track a single Raman band, an analysis termed univariate linear regression, and discard the remaining rich spectral information.[18,19] We have recently shown that this technique may be greatly improved upon with multilinear regression, due to fluctuations in band enhancements relative to one another.[20]

The complexity in quantitative, predictive SERS has led to the adoption of machine learning methods such as partial least squares,[10] support vector machines,[21] and artificial neural networks (ANNs).[22] Of these ANNs have several properties uniquely advantageous for SERS. As a nonlinear method, ANNs are well suited for deviations from Langmuir adsorption dynamics.[23] ANNs also have the universal approximation property that enables them to approximate any latent random variable, an essential property for multiplexed SERS.[24] Finally, they naturally denoise complexly varying signals.[23]

Yet ANNs are not perfectly suited for predicting analyte concentration from maps of SERS spectra. Underlying spatial variation of Raman enhancement and hotspot volume from the SERS sensing surface leads to variance in predictions.[20] Indeed, consider that at low concentrations, analyte molecules will not be uniformly distributed across the surface.[25,26] In this work, we obviate these challenges by employing convolutional neural networks (CNNs). 1D CNNs, which have been shown to perform well on data having spatial relations in a single dimension, such as stock price,[27] electroencephalograms (EEGs),[28] audio signals.[29]

Here, we bundle multiple Raman spectra into a 1D line with channels representing the wavenumber features of each spectrum. This strategy enables the network to learn the underlying distribution of Raman enhancement and hotspot volume within sensor surfaces. Thus, each input is given as a sparse distribution of these latent variables in addition to the analyte information. In a complex biological fluid, we train models to predict concentrations of pyocyanin, an important biomolecule.[30] We demonstrate that this approach significantly improves prediction accuracy, yielding an r^2 of 0.95, compared to the ANN r^2 of 0.89. Further, we demonstrate that this model uses the important spectral information from the analyte and is capable of making reasonable interpolations between trained concentrations.

RESULTS AND DISCUSSION

2-dimensional physically activated chemistry (2PAC) is used to self-assemble high quality surface enhanced Raman scattering (SERS) sensing surfaces. Figure 1a depicts a schematic of the 2PAC assembly, which is a seeded growth of close-packed nanoparticle assemblies. 2PAC is described in more detail elsewhere.[16] Briefly, nanoparticle seeds are driven to a copolymer coated Si electrode by electrophoresis. EDC activates the carboxylic acid functionalized nanospheres, enabling a crosslinking reaction to amine functionalized domains of the copolymer. At the surface, the interaction between the electric double layers of the electrode and the nanoparticles drives electrohydrodynamic (EHD) flow. This lateral, attractive flow entrains nearby particles, forming close-packed nanosphere assemblies. The close proximity of the nanospheres within oligomers gives rise to repeated collisions, enabling a carbodiimide-mediated crosslinking between carboxylic acid groups on adjacent nanoparticles that results anhydride linked gaps of ~0.9 nm.

A scanning electron microscopy (SEM) image of a 2PAC assembled sensing surface is depicted in Figure 1b. One may observe discrete, close-packed assemblies. Importantly, the resonance wavelength of such oligomers is dictated by the number of particles along a given axis. Assembled as they are here, this corresponds primarily to 3-4 particles along a line, which was shown to have a resonance wavelength (for 40 nm spheres) near the excitation wavelength used in this work, 785 nm. Discrete oligomers have greater field enhancements than 2-D close packed assemblies, while still having a relatively dense collection of hotspots for analyte molecules to reside. The reproducibility of the gap spacings due to chemical crosslinking and the rotational invariance of the close-packed oligomers enables the surfaces to be optically uniform within the laser spot size across large sample surfaces.

Raman spectra used to train and validate our models are acquired from concentrations gradients of the biomolecule pyocyanin. To simulate biosensing environments, pyocyanin is dissolved in LB broth, a bacterial nutrient solution. Figure 2 depicts representative Raman spectra of pyocyanin where characteristic Raman bands are observed at 552, 1353, 1602, and 1620 cm^{-1}, among other spectral regions. SERS spectroscopy is performed on the surfaces by acquiring 16 x 24 μm maps with 2 μm spacings between acquisitions. Spectra are acquired for 0.1 s at a laser power of 760 μW at 785 nm with a 1.2 NA water immersion objective.

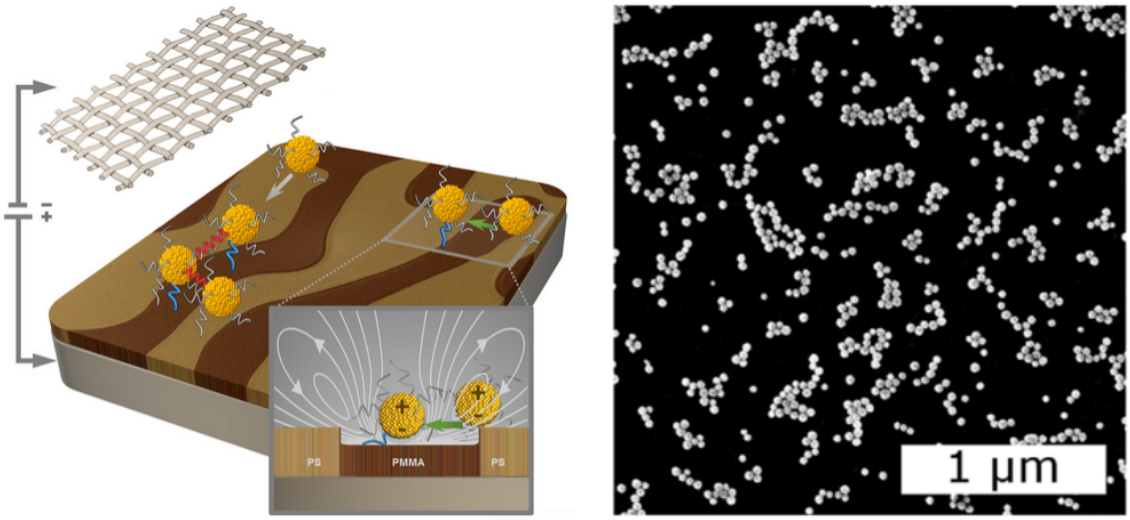

Figure 1. a) Schematic of 2PAC self-assembly. Electrophoresis drives carboxylic acid functionalized nanoparticle "seeds" to collide with the amine functionalized block copolymer coated electrode where EDC crosslinks them to the surface. Inset: seeds drive electrohydrodynamic flow that entrains nearby particles enabling a second EDC activated crosslinking between particles yields anhydride linked two-dimensional close-packed assemblies. b) SEM micrograph of close-packed nanoparticle assemblies.

In this work, we seek to demonstrate that grouping multiple measurements together as inputs into a regression model significantly improves concentration predictions. To this end, we evaluate several methods for quantifying concentration from Raman spectra. A 20/80 test/train split is performed, and the models are evaluated based on its test r^2. Early stopping based on r^2 is used on all neural network models as a regularization method. Principal component analysis (PCA), just fit to the training dataset, is used for all methods to reduce the dimension of the 1011 wavenumber features to 60 features. Analyte hotspot occupation is expected to follow the Langmuir isotherm, which predicts a log-linear relationship between concentration and hotspot occupation. Due to this, all regressions are performed on a log-linear scale with the blank (water) dataset manually set to 10 fold smaller concentration than the next smallest concentration, 0.1 ng/mL.

Figure 3 depicts two models that use one spectra to infer one concentration, partial least squares regression (PLSR) and a multilayer perceptron (MLP). First, we consider PLSR, which is used to give a baseline performance for the problem of inferring analyte concentration from Raman spectra. In Figure 3 a), one may observe an mean squared error of 0.85 and an r^2 of 0.88, indicating significant bias and variance in the predicts. Bias in the predictions is interpreted as deviation from the Langmuir isotherm, while variance indicates fluctuating Raman enhancement and analyte hotspot occupation from the underlying SERS sensing surface. Using a nonlinear model like MLP, deviations from Langmuir adsorption behavior can be captured upon model training. Further, this model more effectively uses the spectral information to infer the Raman

enhancement of each spectra, reducing variance. A mean squared error of 0.74 and r^2 of 0.89 is observed for this model, whose predictions are plotted in Figure 3 b).

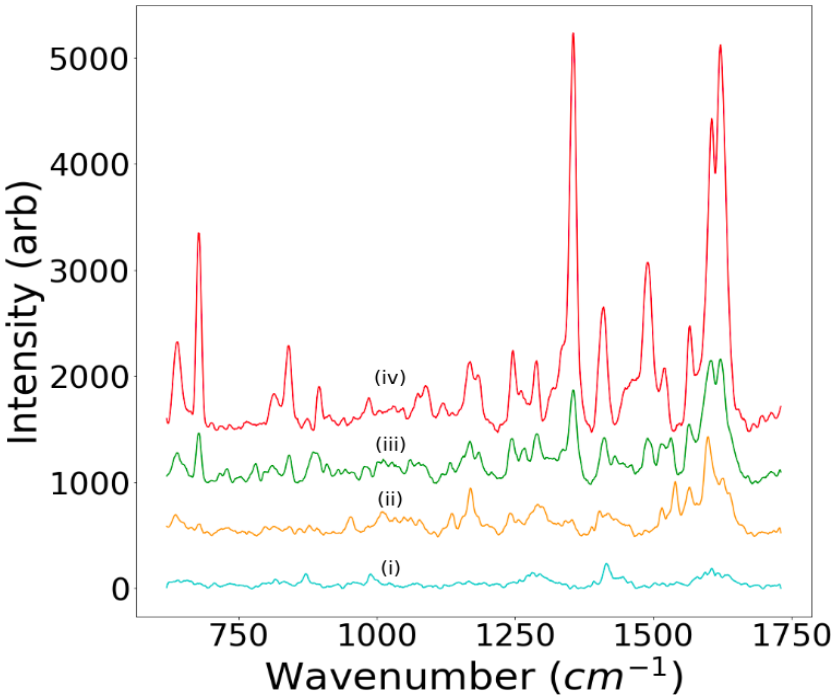

Figure 2 depicts representative Raman spectra acquired from 2PAC assembled surfaces with pyocyanin concentrations of i) 0 ng/mL ii) 100 ng/mL iii) 1 µg/mL and iv) 10 µg/mL. Spectra are offset by 500 units for visual clarity.

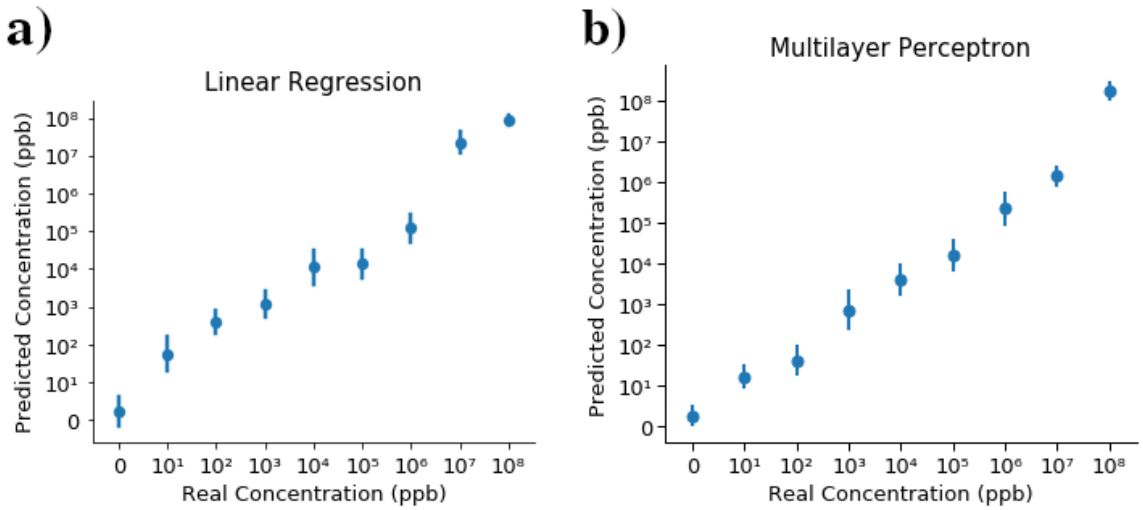

Figure 3. a) depicts the concentration predictions of the PLS model for spectra obtained from the test dataset. b) depicts the concentration predictions of the MLP model for spectra obtained from the test dataset.

Due to the use of a sensing surface, SERS necessarily introduces signal fluctuations that emerge from spot to spot variations in Raman enhancement and hotspot volume. While the MLP seems to be able to infer these parameters to some degree from one spectra, significant improvements to predictions could be made by taking into account the distribution of these fluctuations while making predictions about concentration. Convolutional neural networks (CNNs) are well suited for identifying distributions within pixels of an image. We implement a CNN for concentration quantification, depicted in figure 4, by encoding five spectra as pixels within a one dimensional image, where each pixel has 60 channels to encode the pca components.

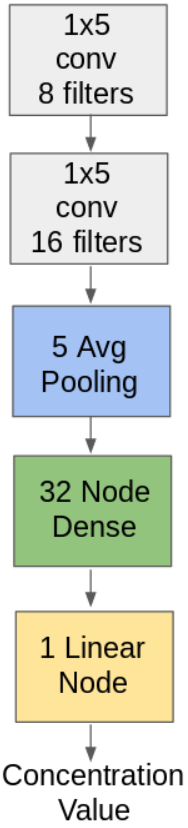

Figure 4. A schematic representation of the convolutional neural network model used in this work.

Figure 5 a) depicts the concentration predictions of the 1D CNN. We find this model achieves a mean squared error of 0.29 and an r^2 of 0.95, significantly better than either the PLSR or MLP models. In the regression problem, interpolation is critical. Often, increased model complexity reduces variance, but at the expense of the ability of the model to interpolate. Yet we find, despite the complexity, the 1D CNN is still capable of making good interpolations. Figure 5 b) is produced by removing two concentrations from the training dataset, 10^2 ng/mL, and 10^5 ng/mL, and plotting the predictions of the test dataset with the concentrations included. We find the model predicts these concentrations with reasonable accuracy.

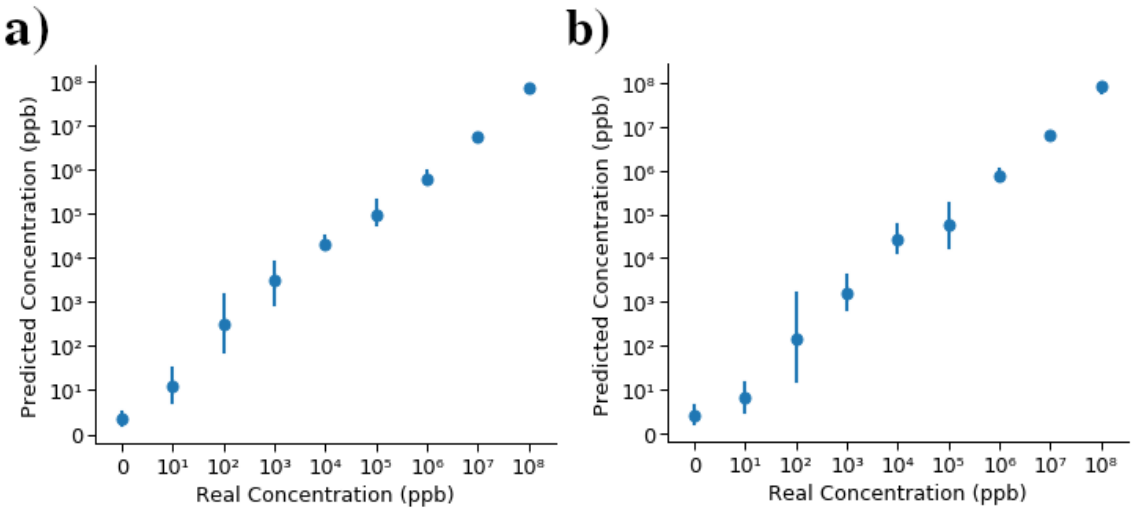

Figure 5. a) depicts the concentration predictions of the CNN model for spectra obtained from the test dataset. b) depicts the concentration predictions of the CNN model for spectra obtained from the test dataset with 10^2 and 10^5 ppb removed from the training dataset.

While challenging, interpreting neural network models is critical to ensuring that decisions are being made using features for which there is a causal relationship with the output. In Raman sensing, this amounts to ensuring that the network is using spectral information associated with pyocyanin vibrations. Here, we implement gradient assisted class activation mapping, gradCAM,[31] to interpret what spectral information is being used. Gradcam identifies network attention by determining how much the output changes with respect to the derivative of the input into the final fully connected layer. We implement this by omitting PCA dimensionality reduction and averaging the gradCAM values in each wavenumber channel over all of the spectra. Thus, we visualize the attention on a given wavenumber value. We find the network uses the 1353, 1602, and 1620 cm^{-1} to make its predictions, corresponding to prominent pyocyanin vibrational energies.

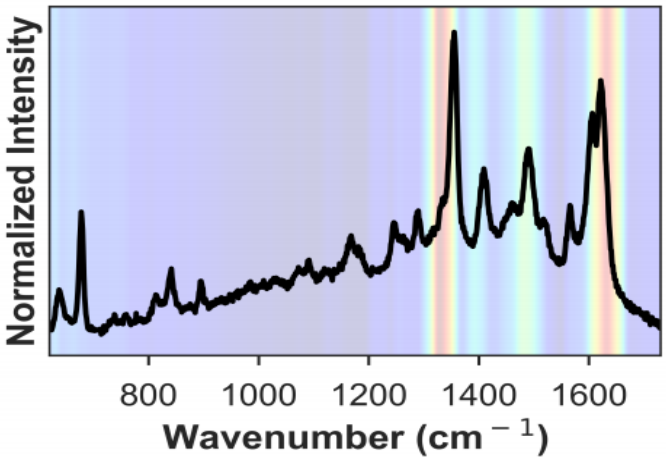

Figure 6 depicts a heat map of the spectral averaged gradCAM score of the wavenumber features. A Raman spectrum is plotted for reference.

CONCLUSION

In this work, we have demonstrated the use of 1D convolutional neural networks (CNNs) to learn the distribution of underlying, sensor based signal fluctuations to reduce variance in concentration predictions. We have shown this method yields an improvement in r^2 from 0.89 to 0.95, for the multilayer perceptron and 1D CNN, respectively. We have shown that the 1D CNN model uses analyte spectral information for its predictions, and the ability of the model to interpolate between concentration values. This method is broadly applicable to any sensing platform where it is unnecessary to predict concentration from each measurement, and where variance arises from latent distributions of intensity enhancement that emerge from spatial variations on the sensor surface.

METHODS

Materials

Random copolymer poly(styrene-co-methyl methacrylate)-α-hydroxyl-ω-tempo moiety (PS-r-PMMA) (Mn = 7400, 59.6% PS) and diblock copolymer poly(styrene-b-methyl methacrylate) (PSb-PMMA) (Mn = 170-b-144 kg mol−1) were purchased from Polymer Source, Inc. (Dorval, Canada). Si(001) wafers with a resistivity of 0.004 ohm-cm were purchased from Virginia Semiconductor (Frederickburg, VA, USA). Hydrofluoric acid (HF) was purchased from Fisher Scientific (Pittsburgh, PA, USA). 2-(N-morpholino)ethanesulfonic acid (MES) 0.1 M buffer, 1-ethyl-3-[3- (dimethylamino)propyl]carbodiimide hydrochloride (EDC), and N-hydroxy sulfosuccinimide (s-NHS) were purchased from Pierce (Rockford, IL, USA). Rhodamine 800, Methylene Blue, dimethyl sulfoxide (DMSO), ethylenediamine, toluene, ethanol, isopropyl alcohol (IPA), potassium carbonate, and 52-mesh Pt gauze foil were all purchased from Sigma-Aldrich (St. Louis, MO, USA). Nanopure deionized water (DI) (18.2 MΩ cm−1) was obtained from a Milli-Q Millipore System.

2-Dimensional Physically Activated Chemical (2PAC) Assembly

Assembly is performed as in previous work. Random PS-b-PMMA block copolymer is spin-coated onto a HF-cleaned (the potential of HF to cause severe injury mandates extreme caution during usage), heavily doped Si wafer and annealed at 198^0 C for three days. The sample is rinsed with toluene and lamella-forming PS-b-PMMA block copolymer is spin-coated onto the sample. PMMA regions are selectively functionalized with amine end groups by immersing the entire substrate in DMSO and then in ethylenediamine/DMSO solution (5% v/v), both for 5 min without rinsing between steps. The surface is rinsed with IPA and dried under nitrogen. Au nanosphere solution (0.1 mg/mL, 3 mL) is added to a 10 mL glass beaker. Freshly prepared s-NHS (20 mM) in a MES (0.1 M) buffer (35 μL) is added to the beaker and swirled. Next, freshly prepared EDC (8 mM) in a MES (0.1 M) buffer (35 μL) is added to the beaker and swirled. The solution then is brought to 60 °C. A 1 cm × 1 cm functionalized copolymer-coated Si substrate is placed into the solution vertically. One millimeter away from the substrate, a 1 cm × 1 cm Pt mesh is placed into the solution vertically. A dc regulated power supply is used to apply a voltage of 1.2 V for 10 min. This process is then repeated with the same substrate and fresh nanosphere solution as described above, but with 25 μL of EDC and s-NHS solution.

Characterization

SEM Images are collected with a Magellan XHR SEM (FEI). Raman spectroscopy measurements are conducted using a confocal Renishaw InVia micro Raman system with a laser excitation wavelength of 785 nm. All measurements are taken at 7.3 μW with exposure of 0.5 s and use a 60× water immersion objective with a 1.2 NA.

ACKNOWLEDGEMENTS

The authors acknowledge the National Science Foundation EECS-1449397 for funding this work. The authors also acknowledge the use of the facilities within the Laser Spectroscopy Facility and the Laboratory for Electron and X-ray Instrumentation (LEXI) Center at the University of California, Irvine. W.J.T. acknowledges funding from a NSF IGERT Fellowship. J.K. acknowledges funding from an Edison STEM fellowship. J. W. acknowledges funding from a UCI UROP fellowship.

REFERENCES

[1] Larkin, P., [Infrared and Raman Spectroscopy; Principles and Spectral Interpretation], Elsevier (2011).
[2] Mosier-Boss, P. and Mosier-Boss, P. A., "Review of SERS Substrates for Chemical Sensing," Nanomaterials 7(6), 142 (2017).
[3] Maier, S. A., [Plasmonics: Fundamentals and Applications], Springer Science & Business Media (2007).
[4] Campione, S., Adams, S. M., Ragan, R. and Capolino, F., "Comparison of electric field enhancements: Linear and triangular oligomers versus hexagonal arrays of plasmonic nanospheres," Opt. Express 21(7), 7957–7973 (2013).
[5] Blackie, E. J., Le Ru, E. C. and Etchegoin, P. G., "Single-Molecule Surface-Enhanced Raman Spectroscopy of Nonresonant Molecules," J. Am. Chem. Soc. 131(40), 14466–14472 (2009).
[6] Hakonen, A., Andersson, P. O., Stenbæk Schmidt, M., Rindzevicius, T. and Käll, M., "Explosive and chemical threat detection by surface-enhanced Raman scattering: A review," Analytica Chimica Acta 893, 1–13 (2015).
[7] Si, K. J., Guo, P., Shi, Q. and Cheng, W., "Self-Assembled Nanocube-Based Plasmene Nanosheets as Soft Surface-Enhanced Raman Scattering Substrates toward Direct Quantitative Drug Identification on Surfaces," Anal. Chem. 87(10), 5263–5269 (2015).
[8] Pang, S., Yang, T. and He, L., "Review of surface enhanced Raman spectroscopic (SERS) detection of synthetic chemical pesticides," TrAC Trends in Analytical Chemistry 85, 73–82 (2016).
[9] Kasera, S., Herrmann, L. O., Barrio, J. del, Baumberg, J. J. and Scherman, O. A., "Quantitative multiplexing with nano-self-assemblies in SERS," Scientific Reports 4, 6785 (2014).
[10] Nguyen, C. Q., Thrift, W. J., Bhattacharjee, A., Ranjbar, S., Gallagher, T., Darvishzadeh-Varcheie, M., Sanderson, R. N., Capolino, F., Whiteson, K., Baldi, P., Hochbaum, A. I. and Ragan, R., "Longitudinal Monitoring of Biofilm Formation via Robust Surface-Enhanced Raman Scattering Quantification of Pseudomonas aeruginosa-Produced Metabolites," ACS Appl. Mater. Interfaces 10(15), 12364–12373 (2018).
[11] Song, B., Yao, Y., Groenewald, R. E., Wang, Y., Liu, H., Wang, Y., Li, Y., Liu, F., Cronin, S. B., Schwartzberg, A. M., Cabrini, S., Haas, S. and Wu, W., "Probing Gap Plasmons Down to Subnanometer Scales Using Collapsible Nanofingers," ACS Nano 11(6), 5836–5843 (2017).
[12] Van Haute, D., Longmate, J. M. and Berlin, J. M., "Controlled Assembly of Biocompatible Metallic Nanoaggregates Using a Small Molecule Crosslinker," Adv. Mater. 27(35), 5158–5164 (2015).
[13] Cha, H., Yoon, J. H. and Yoon, S., "Probing Quantum Plasmon Coupling Using Gold Nanoparticle Dimers with Tunable Interparticle Distances Down to the Subnanometer Range," ACS Nano 8(8), 8554–8563 (2014).
[14] Taylor, R. W., Lee, T.-C., Scherman, O. A., Esteban, R., Aizpurua, J., Huang, F. M., Baumberg, J. J. and Mahajan, S., "Precise Subnanometer Plasmonic Junctions for SERS within Gold Nanoparticle Assemblies Using Cucurbit[n]uril 'Glue,'" ACS Nano 5(5), 3878–3887 (2011).
[15] Chikkaraddy, R., de Nijs, B., Benz, F., Barrow, S. J., Scherman, O. A., Rosta, E., Demetriadou, A., Fox, P., Hess, O. and Baumberg, J. J., "Single-molecule strong coupling at room temperature in plasmonic nanocavities," Nature 535(7610), 127–130 (2016).
[16] Thrift, W. J., Nguyen, C. Q., Darvishzadeh-Varcheie, M., Zare, S., Sharac, N., Sanderson, R. N., Dupper, T. J., Hochbaum, A. I., Capolino, F., Abdolhosseini Qomi, M. J. and Ragan, R., "Driving Chemical

Reactions in Plasmonic Nanogaps with Electrohydrodynamic Flow," ACS Nano 11(11), 11317–11329 (2017).
[17] Nguyen, C. Q., "Machine Learning for SERS Quantitative Detection of Pyocyanin" (2018).
[18] Bodelón, G., Montes-García, V., López-Puente, V., Hill, E. H., Hamon, C., Sanz-Ortiz, M. N., Rodal-Cedeira, S., Costas, C., Celiksoy, S., Pérez-Juste, I., Scarabelli, L., La Porta, A., Pérez-Juste, J., Pastoriza-Santos, I. and Liz-Marzán, L. M., "Detection and imaging of quorum sensing in Pseudomonas aeruginosa biofilm communities by surface-enhanced resonance Raman scattering," Nat Mater 15(11), 1203–1211 (2016).
[19] Qi, G., Jia, K., Fu, C., Xu, S. and Xu, W., "A highly sensitive SERS sensor for quantitative analysis of glucose based on the chemical etching of silver nanoparticles," J. Opt. 17(11), 114020 (2015).
[20] Nguyen, C., Thrift, W., Bhattacharjee, A., Whiteson, K., Hochbaum, A. and Ragan, R., "Robust SERS spectral analysis for quantitative detection of pycocyanin in biological fluids," Biosensing and Nanomedicine X 10352, 1035205, International Society for Optics and Photonics (2017).
[21] Dong, R., Weng, S., Yang, L. and Liu, J., "Detection and Direct Readout of Drugs in Human Urine Using Dynamic Surface-Enhanced Raman Spectroscopy and Support Vector Machines," Anal. Chem. 87(5), 2937–2944 (2015).
[22] Alharbi, O., Xu, Y. and Goodacre, R., "Simultaneous multiplexed quantification of nicotine and its metabolites using surface enhanced Raman scattering," Analyst 139(19), 4820–4827 (2014).
[23] Hassoun, M. H., [Fundamentals of Artificial Neural Networks], MIT Press (1995).
[24] Hornik, K., Stinchcombe, M. and White, H., "Multilayer feedforward networks are universal approximators," Neural Networks 2(5), 359–366 (1989).
[25] Le Ru, E. C., Grand, J., Sow, I., Somerville, W. R. C., Etchegoin, P. G., Treguer-Delapierre, M., Charron, G., Félidj, N., Lévi, G. and Aubard, J., "A Scheme for Detecting Every Single Target Molecule with Surface-Enhanced Raman Spectroscopy," Nano Lett. 11(11), 5013–5019 (2011).
[26] Le Ru, E. C., Meyer, M. and Etchegoin, P. G., "Proof of Single-Molecule Sensitivity in Surface Enhanced Raman Scattering (SERS) by Means of a Two-Analyte Technique," J. Phys. Chem. B 110(4), 1944–1948 (2006).
[27] Tsantekidis, A., Passalis, N., Tefas, A., Kanniainen, J., Gabbouj, M. and Iosifidis, A., "Forecasting Stock Prices from the Limit Order Book Using Convolutional Neural Networks," 2017 IEEE 19th Conference on Business Informatics (CBI) 01, 7–12 (2017).
[28] Tabar, Y. R. and Halici, U., "A novel deep learning approach for classification of EEG motor imagery signals," J Neural Eng 14(1), 016003 (2017).
[29] Lee, J., Park, J., Kim, K. L. and Nam, J., "Sample-level Deep Convolutional Neural Networks for Music Auto-tagging Using Raw Waveforms," arXiv:1703.01789 [cs] (2017).
[30] Thrift, W. J., Bhattacharjee, A., Darvishzadeh-Varcheie, M., Lu, Y., Hochbaum, A., Capolino, F., Whiteson, K., and Ragan, R., "Surface Enhanced Raman Scattering for Detection of *Pseudomonas Aeruginosa* Quorum Sensing Compounds", International Society for Optics and Photonics, Vol. 9550, p 95500B (2015).
[31] Selvaraju, R. R., Cogswell, M., Das, A., Vedantam, R., Parikh, D. and Batra, D., "Grad-CAM: Visual Explanations from Deep Networks via Gradient-based Localization," arXiv:1610.02391 [cs] (2016).